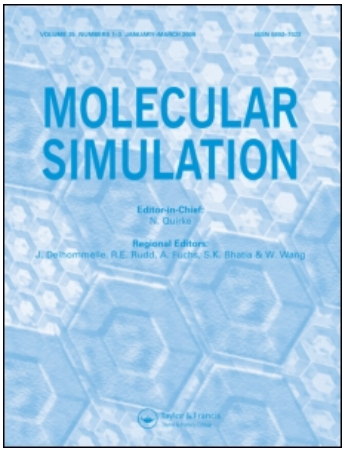

Molecular Simulation
Publication details, including instructions for authors and subscription information:
http://www.informaworld.com/smpp/title~content=t713644482

A grand canonical Monte-Carlo simulation study of water adsorption on a model soot particle

F. Moulin[a]; S. Picaud[a]; P. N. M. Hoang[a]; L. Pártay[b]; P. Jedlovszky[b]
[a] Laboratoire de Physique Moléculaire, UMR CNRS 6624, Faculté des Sciences, La Bouloie, Université de Franche-Comté, Besançon Cedex, France [b] Department of Colloid Chemistry, Institute of Chemistry, Eötvös Loránd University, Budapest, Hungary

To cite this Article Moulin, F. , Picaud, S. , Hoang, P. N. M. , Pártay, L. and Jedlovszky, P.(2006) 'A grand canonical Monte-Carlo simulation study of water adsorption on a model soot particle', Molecular Simulation, 32: 7, 487 — 493
To link to this Article: DOI: 10.1080/08927020600622048
URL: http://dx.doi.org/10.1080/08927020600622048

Molecular Simulation, Vol. 32, No. 7, 15 June 2006, 487–493

Taylor & Francis
Taylor & Francis Group

A grand canonical Monte-Carlo simulation study of water adsorption on a model soot particle

F. MOULIN†, S. PICAUD†*, P. N. M. HOANG†, L. PÁRTAY‡ and P. JEDLOVSZKY‡

†Laboratoire de Physique Moléculaire, UMR CNRS 6624, Faculté des Sciences, La Bouloie, Université de Franche-Comté, Besançon Cedex F-25030, France
‡Department of Colloid Chemistry, Institute of Chemistry, Eötvös Loránd University, Pázmány Péter stny. 1/a, Budapest H-1117, Hungary

(Received November 2005; in final form February 2006)

The grand canonical Monte-Carlo (GCMC) method is used to simulate the adsorption of water molecules on a spherical soot particle. Soot is modelled by graphite-type layers arranged in an onion-like structure. The calculated water adsorption isotherm at 298 K exhibits two plateaus, corresponding to the filling of the internal core of the soot particle and to the three-dimensional condensation of the water molecules around it, respectively. Moreover, no wetting of the external soot surface is evidenced. The results of these simulations can help in interpreting experimental isotherms of water adsorbed on aircraft soot.

Keywords: Grand canonical Monte-Carlo; Soot; Water adsorption; Graphite-type layers

1. Introduction

In the last few years, there has been an increasing interest on the adsorption of water molecules on soot particles emitted by aircraft. Indeed, time evolution of airplane condensation trails can lead to the formation of artificial cirrus clouds [1,2]. These artificial clouds, together with natural cirrus clouds, may have a large impact on the chemistry of the upper troposphere/lower stratosphere (UTLS) by providing active surfaces for heterogeneous chemical processes such as, e.g. the conversion of HNO_3 to NO_x [3,4], or the photo-oxidation of adsorbed volatile organic compounds to HO_x [5]. Moreover, cirrus clouds may also contribute to climate changes by allowing solar radiation to heat the earth surface but absorbing terrestrial radiation which adds to "greenhouse" warming [6].

In addition to the impact of aircraft emissions in the UTLS, recent questions also arose on the influence of soot particles emitted by airplanes near airports on the human health. Indeed, due to their very small size, soot particles can likely be inhaled with possible worsening symptoms of respiratory conditions in elderly people and children. The chemical composition of these soot particles has also been linked to death from lung cancer and heart diseases [7]. Moreover, these particles provide nucleation sites for both organic liquid and moisture droplets. Aggregation of particles results in sufficiently large droplets that may or may not be removed from the atmosphere because of the turbulent mixing within the inversion layer. These droplets can be deposited on houses, cars, swimming pools, etc. and thus impact our close environment, especially in humid or foggy conditions [8].

These environmental interests have motivated the characterisation of aircraft combustion soot by means of different techniques. Recently, transmission electron microscopy (TEM) studies have shown that soot is made of nanocrystallites containing graphite-type layers arranged in an onion-like structure forming quasi-spherical carbon nanoparticles with diameters in the range of 200–500 Å [9,10]. Thus, soot is characterised by nanopores of various sizes, which are observed inside the structure of each carbon nanoparticle (pores of small size), as well as between agglomerated nanoparticles (pores of larger sizes). Additional results of Raman spectroscopy measurements have revealed that the graphite layers are partially oxidised and thus contain a certain number of hydrophilic sites [10]. Thermodynamic measurements of water adsorption isotherms confirmed that soot particles, unlike pure graphite, can acquire a substantial amount of water molecules around 300 K [11,12].

Although, a lot of both experimental [13–16] and theoretical [17–24] works have been recently published

*Corresponding author. Email: sylvain.picaud@univ-fcomte.fr

Molecular Simulation
ISSN 0892-7022 print/ISSN 1029-0435 online © 2006 Taylor & Francis
http://www.tandf.co.uk/journals
DOI: 10.1080/08927020600622048

on the adsorption of water in porous carbon (see, e.g. the recent review by Gubbins *et al.* [25]), rather few studies have been reported so far on soot particles specifically, despite their atmospheric importance. Thus, a detailed theoretical understanding of the water nucleation dynamics on soot at the molecular level remains challenging. In a series of previous papers [26–30], we have combined quantum calculations and classical molecular dynamics simulations to model the interaction between water molecules and a partially oxidised soot particle. This soot particle was modelled by anchoring several COOH or OH active groups on the face or on the edges of a large graphite cluster. These calculations have shown that the sites anchored on the edge of the graphite cluster are more attractive for water than the sites anchored on its face [28,29], and that the water adsorption energy on the COOH group is twice the value calculated on an OH group, indicating preferential adsorption of water on graphite surfaces containing COOH rather than OH groups [26,27,29,30]. Indeed, the formation of two hydrogen bonds between a COOH group and the adsorbed water molecules results in a strong trapping of several water molecules on these groups, which then become nucleation centers for other water molecules that can form larger aggregates on the soot [26,27].

In addition to the presence of such hydrophilic sites, the influence of the soot morphology on the adsorption of water needs also to be taken into account. In the present paper, we use the grand canonical Monte-Carlo (GCMC) method [31] to investigate the adsorption of water molecules on a model soot particle of spherical shape at 298 K, i.e. conditions characteristics of the ground altitude. The GCMC method allows us to simulate a real adsorption experiment where the temperature and the chemical potential of the water molecules (or the pressure of the corresponding gas) are kept constant [25,31,32]. This method is used to calculate the water adsorption isotherm at 298 K, and the distributions of the binding energy of the water molecules corresponding to various values of the water chemical potential.

2. Numerical details

2.1 The soot model

The soot particle modelled at atomistic resolution has been generated by replicating a small cluster of carbon atoms on concentric spheres arranged in an onion-like structure. This small cluster containing 19 carbon atoms is made of 5 fused benzene rings and will be referred below as the C_{19} unit. 113 of these C_{19} units have been randomly scattered on the surface of four concentric spheres of radii ranging from 9.8 to 20.0 Å. The separation of two successive spheres is thus equal to 3.4 Å, i.e. close to the distance between two layers in pure graphite [33]. For the scattering of the C_{19} units on the surface of these spheres, a minimum distance of 3.80 Å has been imposed between

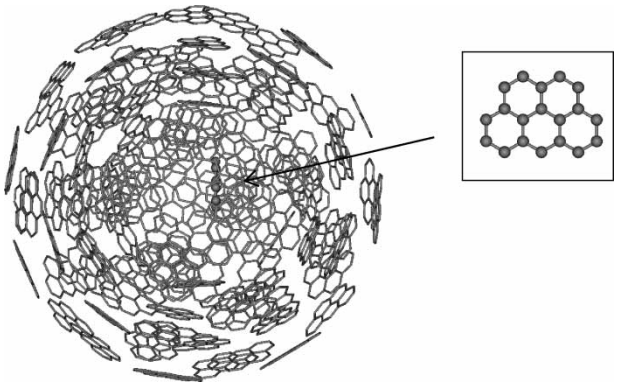

Figure 1. Geometry of the soot particle used in the GCMC calculations. It is made of 113 small C_{19} units of 19 carbon atoms randomly arranged on the surface of four concentric spheres (see text) and one additional C_{19} unit located in the middle of the system. The C_{19} unit is shown in the inset.

the nearest neighbouring carbon atoms of two adjacent units. Note that this distance has been chosen to be slightly larger than the Lennard-Jones (LJ) parameter for the dispersion–repulsion interaction between two carbon atoms [33]. Also, the relative orientation of two adjacent C_{19} units has been randomly distributed. Finally, an additional C_{19} unit has also been included in the internal core of the system (i.e. at the center of the smallest sphere), and the soot particle thus contains 2166 carbon atoms. The schematic structure of the C_{19} basic unit and the soot particle built up by it in the above way and used in the simulations is shown in figure 1.

Although, the carbon system constructed this way is quite small (its diameter is equal to about 40 Å), it can been considered as a realistic model representing the morphology of a soot particle because it contains most of the geometric ingredients characterising soot emitted by aircrafts or collected in flames [9,34,35], i.e. graphite-type layers arranged in an onion-like structure forming quasi-spherical particles and the internal core made of a disordered arrangement of small graphite clusters. Note however, that this model does not include chemical defects such as oxygen containing sites, nor hydrogen atoms which could be bound to the peripheral carbon atoms.

It should also be noted that much larger soot particles can also be constructed using the same method, which is not limited in size, but these large particles are characterised by large volume and surface leading to the possible adsorption of a huge number of water molecules in the GCMC simulations. The present soot particle should then be considered as a good compromise between realistic model and tractable computer time calculations.

2.2 Interaction potentials

The TIP4P potential [36] is used to model water–water interactions. It is a four-site model including a dispersion–repulsion interaction site located on the oxygen atom and three point charges q_i located on the hydrogen atoms and on an additional site displaced by 0.15 Å with respect to

the oxygen atom. Thus, the interaction between two water molecules w_a and w_b is written as a sum of a LJ term plus the Coulomb interactions between the partial charges, as

$$U_{w_a,w_b} = 4\epsilon_{OO}\left[\left(\frac{\sigma_{OO}}{r_{O_a,O_b}}\right)^{12} - \left(\frac{\sigma_{OO}}{r_{O_a,O_b}}\right)^{6}\right] + \frac{1}{4\pi\epsilon_0}\sum_{ij}\frac{q_{i_a}q_{j_b}}{r_{i_a,j_b}}, \quad (1)$$

where $\epsilon_{OO} = 0.648\,\text{kJ/mol}$ and $\sigma_{OO} = 3.1536\,\text{Å}$ are the LJ parameters for the O–O interaction. Here, r_{O_a,O_b} denotes the distance between the oxygen pertaining to molecules w_a and w_b, respectively, and r_{i_a,j_b} represents the distance between the charged sites of the two interacting molecules.

The interaction between the water molecules and the soot particle consists of the pairwise additive sum of LJ terms $U_{w,c}$ between the carbon atoms and the oxygen atoms of water, only. It is written as

$$U_{w,c} = 4\epsilon_{OC}\sum_{a=1}^{N_w}\sum_{\alpha=1}^{N_C}\left[\left(\frac{\sigma_{OC}}{r_{a,\alpha}}\right)^{12} - \left(\frac{\sigma_{OC}}{r_{a,\alpha}}\right)^{6}\right], \quad (2)$$

where $r_{a,\alpha}$ represents the interatomic distance between the O atom of the water molecule a and the αth carbon atom, whereas $\epsilon_{OC} = 0.421\,\text{kJ/mol}$ and $\sigma_{OC} = 3.280\,\text{Å}$ are the LJ parameters for the O–C interaction. These parameters were obtained by the usual Lorentz-Berthelot combining rules between the TIP4P parameters, and the values $\sigma_{CC} = 3.40\,\text{Å}$ and $\epsilon_{CC} = 0.273\,\text{kJ/mol}$, for carbon–carbon interactions [37]. Note that, for consistency with the TIP4P model, no carbon–hydrogen LJ term was introduced, although such a contribution could influence the water orientation in the water–graphite interfacial region [38].

Moreover, no carbon–carbon interactions have been taken into account in the present approach, implying that our soot particle is regarded as an indeformable rigid body in the simulations. In addition, no polarisation effects have been considered in the present approach, although the TIP4P potential already contains some mutual polarisation effects between water molecules taken into account in an average way through its parametrisation. Moreover, it has been recently demonstrated that these polarisation effects have only a small influence on the results of water adsorption on carbon systems of high symmetry (e.g. nanotubes) [39,40]. A spherical cut-off with a radius of 12.5 Å has been adopted to calculate all interactions. This cut-off is actually large enough to make large distance contributions negligible, and no long range correction was necessary to ensure the convergence of the calculations.

2.3 The GCMC simulations

Monte-Carlo simulations of the hydrated soot particle have been performed on the grand canonical (μ, V, T) ensemble at 298 K. The edge length of the cubic simulation box has been set to 50.0 Å; standard periodic boundary conditions have been applied. The simulations have been performed with 27 different values of the B parameter, related to the excess chemical potential of the water molecules through the relation [41]

$$\mu_{ex} = k_B T(B - \ln\langle N\rangle), \quad (3)$$

where k_B is the Boltzmann constant, T is the absolute temperature and $\langle N\rangle$ is the mean number of the water molecules in the system. The B values considered cover the range from -2.00 to 6.00, corresponding to the μ range between -44.1 and -24.3 kJ/mol (μ being the full chemical potential of water including also the ideal gas term). The values of B, $\langle N\rangle$ and μ corresponding to the simulations are collected in table 1.

The simulations have been done using the program MMC [42]. Particle displacement and insertion/deletion steps have been performed in an alternating order. In a particle displacement step, a water molecule has been randomly translated by not more than 0.25 Å and rotated around a randomly chosen space-fixed axis by not more than 15°. In selecting the water molecule to be displaced preferential sampling has been used, i.e. molecules located closer to the centre of the soot particle have been selected for move with higher probabilities. In an insertion/deletion trial, either a randomly chosen water molecule has been removed from the system or an extra water molecule has been added. Insertion and deletion attempts have been done with equal probability. In order to improve sampling efficiency water insertions have been performed using the

Table 1. B and μ values (the latter in kJ/mol) corresponding to the simulations performed.

B	μ	$\langle N\rangle$
−2.0000	−44.1196	1.0309
−1.0000	−41.6427	1.4385
−0.9600	−41.5437	1.6515
−0.8800	−41.3455	2.7868
−0.8400	−41.2464	83.6384
−0.8300	−41.2217	100.3135
−0.8200	−41.1969	111.2728
−0.8100	−41.1722	110.8931
−0.8000	−41.1474	110.0980
−0.7000	−40.8997	114.1308
−0.6000	−40.6520	119.1948
−0.5000	−40.4043	121.1381
−0.4750	−40.3424	122.5978
−0.4500	−40.2805	123.7947
−0.4000	−40.1566	124.2879
−0.3800	−40.1071	125.8225
−0.3500	−40.0328	125.6667
−0.3400	−40.0080	126.7903
−0.3300	−39.9833	127.5748
−0.3000	−39.9089	3165.9663
−0.2600	−39.8090	3176.0698
−0.2200	−39.7100	3181.8652
−0.2000	−39.6612	3195.3127
0.0000	−39.1658	3233.4695
2.0000	−34.2121	3573.4360
4.0000	−29.2500	3828.4204
6.0000	−24.3045	4029.6816

For each B value, the average number of water molecules $\langle N\rangle$ calculated with the GCMC method is also given.

cavity biased method [43,44]. Thus, the extra water molecule has only been attempted to be inserted into empty spherical cavities of the radius of at least 2.5 Å. Cavities have been searched for along a $100 \times 100 \times 100$ grid. The probability of finding a suitable cavity P_{cav}, required for removing the bias of the sampling through the acceptance criterion [43,44] has been calculated as the ratio of the number of cavities found and grid points considered. The ratio of the successful and attempted moves has resulted in about 30% and 0.2–0.5% for the particle displacement and insertion/deletion moves, respectively.

The systems have been equilibrated by performing 7×10^8 Monte-Carlo steps. The results have then been averaged over 5×10^8 equilibrium configurations, sampled in the production phase of the simulations. For the systems characterised by the B values of -0.7 and -0.26, 5000 of these equilibrium configurations, separated by 10^5 Monte-Carlo steps each have been saved for the calculation of the energy distributions.

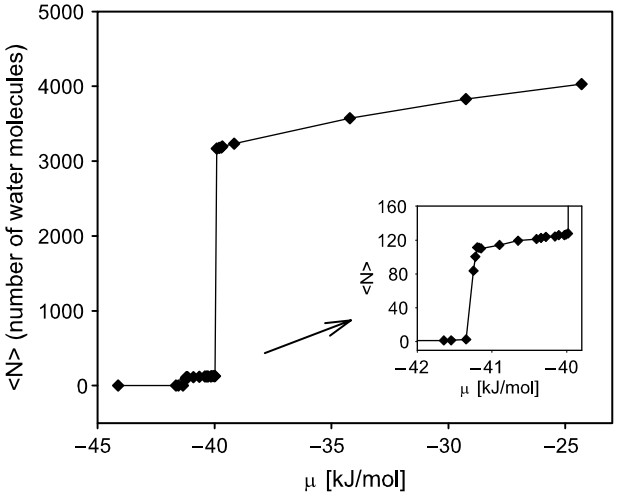

Figure 2. Water adsorption isotherm on the soot particle as a function of the water chemical potential at 298 K. The inset shows the region of the first plateau on a magnified scale.

3. Results and discussion

The adsorption isotherm of water on the soot particle is shown in figure 2 as a function of the water chemical potential as obtained from our simulations. The numerical values of this isotherm are collected in table 1. The isotherm departs from zero at about -41.5 kJ/mol, indicating that below this chemical potential value practically no water is adsorbed on the soot. Then the isotherm exhibits a rapid increase around -41.2 kJ/mol, followed by a plateau in the μ range between about -41 and -40 kJ/mol, indicating the presence of about 120 adsorbed water molecules in the system. (This part of the obtained isotherm is shown on a magnified scale in the inset of figure 2.) Finally, at about -40 kJ/mol the isotherm exhibits another step, ending up in a second, slightly sloped plateau that corresponds to the presence of 3000–4000 water molecules in the system. This plateau evidences the condensation of the water molecules that fill the entire simulation box above -40 kJ/mol.

In order to interpret the details of the obtained isotherm, we present on figure 3 four snapshots of the systems corresponding to different parts of the isotherm. It should be noted that these snapshots are taken during the simulations and they only correspond to an instantaneous view of the system. As a consequence, the corresponding number of water molecules shown in these snapshots may differ from the average value $\langle N \rangle$ given in table 1, especially for low μ values. The first snapshot shown (see figure 3a) corresponds to the first jump of the isotherm, when the soot particle adsorbs only about 15 water molecules. These water molecules are located in the inner core of the soot and form a cluster. To show this, the carbon atoms of the C_{19} unit located in the inner core of the soot particle are represented by balls on the snapshot: the adsorbed water molecules are located on one side of this unit. When increasing the value of μ, water molecules adsorb also on the other side of this C_{19} unit (figure 3b). Then, water entirely fill the interior of the soot particle by adsorbing also between the onion-like outer shells, as shown in figure 3c. It is evident from these snapshots that the adsorbed water molecules are not distributed randomly inside the soot particle; instead they show a strong tendency of clustering. This finding indicates that the driving force of the adsorption of water inside the soot particle partly comes from the attraction of the already adsorbed water molecules. In order to confirm this, we have calculated the distribution of the interaction energy of a water molecule with other waters ($U_{w,w}$) and with the carbon atoms of the system ($U_{w,c}$) for two typical values of the water chemical potential, i.e. $\mu = -40.90$ kJ/mol (filling up the soot particle) and $\mu = -39.81$ kJ/mol (liquid water around the soot particle). The obtained distributions are shown in figure 4. At the low μ value considered, the distribution of the energy between a water molecule and other waters $P(U_{w,w})$ shows a single, rather symmetric peak centered around -72 kJ/mol. On the contrary, the distribution of the energy between a water and the carbon atoms of the soot particle $P(U_{w,c})$ is asymmetric. The position of its maximum at -9.2 k J/mol is much smaller in magnitude than that of $P(U_{w,w})$, and confirms that the adsorption of water inside the soot is mainly driven by the water–water interactions. These interactions lead to the formation of water clusters even at low μ values, which cannot evaporate due to the presence of the surrounding carbon atoms in the internal core of the soot particle. Such a mechanism seems similar to the one calculated in carbon nanopores of small diameters [24].

In the case of the higher μ value, i.e. when liquid water condenses around the soot particle, the distribution $P(U_{w,w})$ exhibits a single, large peak centered around -84 kJ/mol, and is very similar to the distribution obtained in pure liquid TIP4P water [36]. As expected, the distribution energy $P(U_{w,c})$ for $\mu = -39.81$ kJ/mol is characterised by two peaks, a small one around -9 kJ/mol, corresponding to the water molecules adsorbed inside the soot particle, and a high

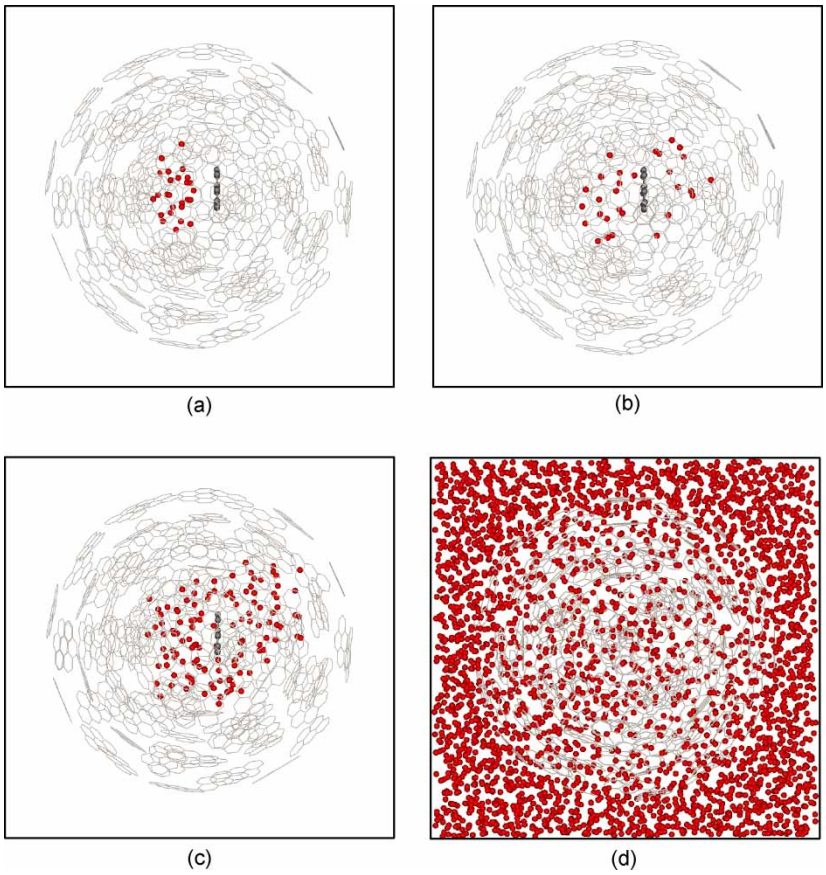

Figure 3. Configurations of water molecules adsorbed at 298 K on the soot particle corresponding to different parts of the isotherm. The oxygen atoms of water are represented as circles, and the hydrogen atoms have been masked for clarity. The carbon atoms of the C_{19} unit located inside the soot particle are also represented as grey circles.

and narrow peak close to zero, corresponding to the molecules of liquid water around the soot.

In the second plateau of the isotherm water condenses to a liquid, as shown in figure 3d, without previously wetting the outer surface of the soot particle. Indeed, no additional plateau is evidenced by the simulations between the filling of the soot particle and the condensation of liquid water. Also, wetting of the outer surface of the soot particle cannot be evidenced either by the shape of the calculated isotherm or by a careful examination of snapshots taken for the μ values ranging from -39.98 to -39.91 kJ/mol, i.e. around the second step of the isotherm.

It is not straightforward to compare the present results with the scarce experimental findings concerning the adsorption of water molecules on soot emitted by aircrafts around 300 K [11,12]. Indeed, our model of the soot particle is rather simple when compared to real soot, although it contains its geometrical ingredients. However, we can explain several features of the experimental data

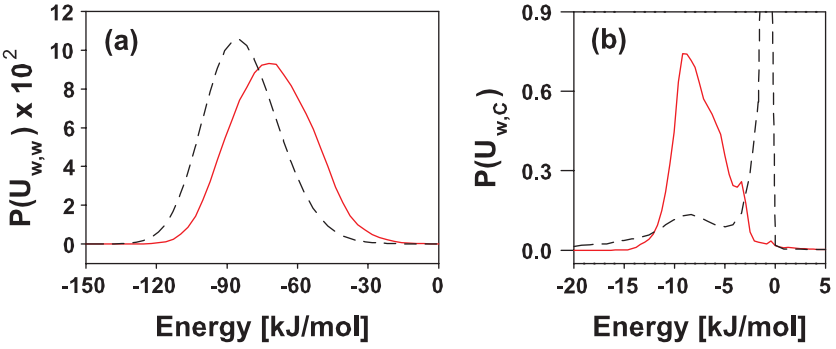

Figure 4. Distribution of the energy of (a) water–water ($U_{w,w}$) and (b) water–carbon ($U_{w,c}$) interaction of a single water molecule for two typical values of the water chemical potential, i.e. $\mu = -40.90$ kJ/mol (full curves) and $\mu = -39.81$ kJ/mol (dashed curves). Note that the main peak in the distribution of water–carbon energy for $\mu = -39.81$ kJ/mol has been cut-off since it corresponds to liquid water molecules having negligible interaction with the soot particle.

[11,12]. Clearly, the first step of the experimental isotherm (observed at low pressure) should correspond to the filling up of the soot particles, as calculated at low μ values, with an aggregation process for the water molecules similar to that reported in theoretical and experimental works on carbon nanopores [25]. At the other end of the simulated isotherm (i.e. at high μ values), the condensation of liquid water corresponds to the saturation of the experimental isotherm at high pressures. On the other hand, features of the experimental data at intermediate pressures are not completely reproduced by the present simulations. Indeed, the slope of the experimental isotherm in this intermediate region has been related to the presence of chemical defects (mainly oxygen containing species), to pore filling, and to adsorption on the external soot surface.

It has been shown that chemical defects (e.g. COOH groups), when present at the surface of nanocrystallites of graphite, can act as nucleation centers for water adsorption [26,27]. Also, recent GCMC calculations have shown that a large amount of water molecules can be adsorbed in graphitic pores or slit of nanometric sizes [25]. Thus, the missing feature of our model can either be attributed to the presence of chemical defects at the outer surface of the soot particle, or/and to the presence of external grooves located between soot particles that approach each other closely. The clarification of this point requires further simulations with accordingly improved models of the system. Work in this direction is currently in progress.

Acknowledgements

This work has been supported by the Hungarian–French Intergovernmental Science and Technology Program (BALATON) under project number F-33/04, and partly also by the Hungarian OTKA Foundation under project No. T049673. Moulin, Picaud and Hoang also thank the French "Agence de l'Environnement et de la Maîtrise de l'Energie (ADEME)" for its financial support through the PRIMEQUAL2-PREDIT program (No. 04 06 C0047). Jedlovszky is a Békésy György Fellow of the Hungarian Ministry of Education, which is gratefully acknowledged.

References

[1] Y. Chen, S.M. Kreidenweiss, L.M. McInnes, D.C. Rogers, P.J. DeMott. Single particle analyses of ice nucleating aerosols in the upper troposphere and lower stratosphere. *Geophys. Res. Lett.*, **25**, 1391 (1998).

[2] P.J. DeMott, Y. Chen, S.M. Kreidenweiss, L.M. McInnes, D.C. Rogers, D.E. Sherman. Ice formation by black carbon particles. *Geophys. Res. Lett.*, **26**, 2429 (1999).

[3] D.A. Hauglustaine, B.A. Ridley, S. Solomon, S. Hess, S. Madronich. HNO_3/NO_x ratio in the remote troposphere during MLOPEX 2: Evidence for nitric acid reduction on carbonaceous aerosols? *Geophys. Res. Lett.*, **23**, 2609 (1996).

[4] C.A. Rogaski, D.M. Golden, L.R. Williams. Reactive uptake and hydration experiments on amorphous carbon treated with NO_2, SO_2, O_3, HNO_3, and H_2SO_4. *Geophys. Res. Lett.*, **24**, 381 (1997).

[5] J.P.D. Abbatt. Interactions of atmospheric trace gases with ice surfaces: adsorption and reaction. *Chem. Rev.*, **103**, 4783 and references therein (2003).

[6] M.A. Zondlo, P.K. Hudson, A.J. Prenni, M.A. Tolbert. Chemistry and microphysics of polar stratospheric clouds and cirrus clouds. *Annu. Rev. Phys. Chem.*, **51**, 473 (2000).

[7] C.A. Pope, R.T. Burnett, M.J. Thun, E.E. Calle, D. Krewski, K. Ito, G.D. Thurston. Lung Cancer, Cardiopulmonary Mortality, and Long-term Exposure to Fine Particulate Air Pollution. *J. Am. Med. Assoc.*, **287**, 1132 (2002).

[8] A.K. Virtanen, J.M. Ristimäki, K.M. Vaaraslahti, J. Keskinen. Effect of Engine Load on Diesel Soot Particles. *Environ. Sci. Technol.*, **38**, 2551 (2004).

[9] O.B. Popovicheva, N.M. Persiantseva, M.E. Trukhin, G.B. Rulev, N.K. Shonija, Y.Y. Buriko, A.M. Starik, B. Demirdjian, D. Ferry, J. Suzanne. Experimental characterization of aircraft combustor soot: microstructure, surface area, porosity and water adsorption. *Phys. Chem. Chem. Phys.*, **2**, 4421 (2000).

[10] O.B. Popovicheva, N.M. Persiantseva, B.V. Kuznetsov, N.K. Rakhmanova, N.K. Shonija, J. Suzanne, D. Ferry. Microstucture and water adsorbability of aircraft combustor soots and kerosene flame soots: Toward an aircraft-generated soot laboratory surrogate. *J. Phys. Chem. A.*, **107**, 10046 (2003).

[11] O.B. Popovicheva, M.E. Trukhin, N.M. Persiantseva, N.K. Shonija. Water adsorption on aircraft-combustor soot under young plume conditions. *Atmosph. Environ.*, **35**, 1673 (2001).

[12] D. Ferry, J. Suzanne, S. Nitsche, O.B. Popovicheva, N.K. Shonija. Water adsorption and dynamics on kerosene soot under atmospheric conditions. *J. Geophys. Res.*, **107**, 4734 (2002).

[13] I.I. Salame, T.J. Bandosz. Experimental study of water adsorption on activated carbons. *Langmuir*, **15**, 587 (1999).

[14] K. Kaneko, Y. Hanzawa, T. Iiyama, T. Kanda, T. Suzuki. Cluster mediated water adsorption on carbon nanopores. *Adsorption*, **5**, 7 (1999).

[15] E. Bekyarova, Y. Hanzawa, K. Kaneko, J. Silvestre-Albero, A. Sepulveda-Escribano, F. Rodriguez-Reinoso, D. Kasuya, M. Yudasaka, S. Iijima. Cluster-mediated filling of water vapor in intratube and interstitial nanospaces of single-wall carbon nanohorns. *Chem. Phys. Lett.*, **366**, 463 (2002).

[16] T. Ohba, H. Kanoh, K. Kaneko. Affinity transformation from hydrophilicity to hydrophobicity of water molecules on the basis of adsorption of water in graphitic nanopores. *J. Am. Chem. Soc.*, **126**, 1560 (2004).

[17] E.A. Müller, L.F. Rull, L.F. Vega, K.E. Gubbins. Adsorption of water on activated carbons : a molecular simulation study. *J. Phys. Chem.*, **100**, 1189 (1996).

[18] E.A. Müller, K.E. Gubbins. Molecular simulation study of hydrophilic and hydrophobic behavior of activated carbon surfaces. *Carbon*, **36**, 1433 (1998).

[19] C.L. McCallum, T.J. Bandosz, S.C. McGrother, E.A. Müller, K.E. Gubbins. A molecular model for adsorption of water on activated carbon: comparison of simulation and experiment. *Langmuir*, **15**, 533 (1999).

[20] E.A. Müller, F.R. Hung, K.E. Gubbins. Adsorption of water vapor-methane mixtures on activated carbons. *Langmuir*, **16**, 5418 (2000).

[21] M. Jorge, C. Schumacher, N.A. Seaton. Simulation study of the effect of the chemical heterogeneity of activated carbon on water adsorption. *Langmuir*, **18**, 9296 (2002).

[22] M. Jorge, N.A. Seaton. Long-range interactions in Monte Carlo simulation of confined water. *Mol. Phys.*, **100**, 2017 (2002).

[23] A. Striolo, A.A. Chialvo, K.E. Gubbins, P.T. Cummings. Water in carbon nanotubes: Adsorption isotherms and thermodynamic properties from molecular simulation. *J. Chem. Phys.*, **122**, 234712 (2005).

[24] J.C. Liu, P.A. Monson. Does water condense in carbon pores? *Langmuir*, **21**, 10219 (2005).

[25] J.K. Brennan, T.J. Bandosz, K.T. Thomson, K.E. Gubbins. Water in porous carbons. *Colloids Surf. A*, **187–188**, 539 (2001).

[26] S. Hamad, J.A. Mejias, S. Lago, S. Picaud, P.N.M. Hoang. A theoretical study of the adsorption of water on a model soot surface. *J. Phys. Chem. B*, **108**, 5405 (2004).

[27] S. Picaud, P.N.M. Hoang, S. Hamad, J.A. Mejias, S. Lago. A theoretical study of the adsorption of water on a model soot surface. II. Molecular dynamics simulations. *J. Phys. Chem. B*, **108**, 5410 (2004).

[28] B. Collignon, P.N.M. Hoang, S. Picaud, J.C. Rayez. Ab initio study of the water adsorption on hydroxylated graphite surfaces. *Chem. Phys. Lett.*, **406**, 431 (2005).
[29] B. Collignon, P.N.M. Hoang, S. Picaud, J.C. Rayez. Clustering of water molecules on model soot particles: an ab initio study. *Comp. Lett.*, **4** (2005) in press.
[30] S. Picaud, B. Collignon, P.N.M. Hoang, J.C. Rayez. A Molecular Dynamics Simulations study of the water adsorption on hydroxylated graphite surface. *J. Phys. Chem.*, (2006) Submitted.
[31] M.P. Allen, D.J. Tildesley. *Computer Simulations of Liquids*, Clarendon, Oxford (1987).
[32] J. Puibasset, R.J.M. Pellenq. Water adsorption in disordered mesoporous silica (Vycor) at 300 K and 650 K: A Grand Canonical Monte Carlo simulation study of hysteresis. *J. Chem. Phys.*, **122**, 094704 (2005).
[33] A.V. Shevade, S. Jiang, K.E. Gubbins. Adsorption of water-methanol mixtures in carbon and alumino-silicate pores: a molecular simulation study. *Mol. Phys.*, **97**, 1139 (1999).
[34] F. Douce. PhD Thesis. Orléans, France. (2001)
[35] D. Ferry, private communication., (2005).
[36] W.L. Jorgensen, J. Chandrasekhar, J.F. Madura, R.W. Impey, M.L. Klein. Comparison of simple potential functions for simulating liquid water. *J. Chem. Phys.*, **79**, 926 (1983).
[37] S.J. Stuart, A.B. Tutein, J.A. Harrison. A reactive potential for hydrocarbons with intermolecular interactions. *J. Chem. Phys.*, **112**, 6472 (2000).
[38] A. Pertsin, M. Grunze. Water-graphite interaction and behavior of water near the graphite surface. *J. Phys. Chem. B*, **108**, 1357 (2004).
[39] J.H. Walther, R. Jaffe, T. Halicioglu, P. Koumoutsakos. Carbon nanotubes in water: structural characteristics and energetics. *J. Phys. Chem. B*, **105**, 9980 (2001).
[40] F. Moulin, S. Picaud, M. Devel. Molecular dynamics simulations of polarizable nanotubes interacting with water. *Phys. Rev. B*, **71**, 165401 (2005).
[41] D.J. Adams. Grand canonical ensemble Monte Carlo for a Lennard-Jones fluids. *Mol. Phys.*, **29**, 307 (1975).
[42] M. Mezei. MMC program, URL: http://fulcrum.physbio.mssm.edu/~mezei/mmc
[43] M. Mezei. A cavity-biased (T,V, mu) Monte Carlo method for the computer simulation of fluids. *Mol. Phys.*, **40**, 901 (1980).
[44] M. Mezei. Grand-canonical ensemble Monte Carlo study of dense liquid Lennard-Jones, soft spheres and water. *Mol. Phys.*, **61**, 565 (1987), Erratum: ibid **67**, 1207 (1989).